Supplementary Information

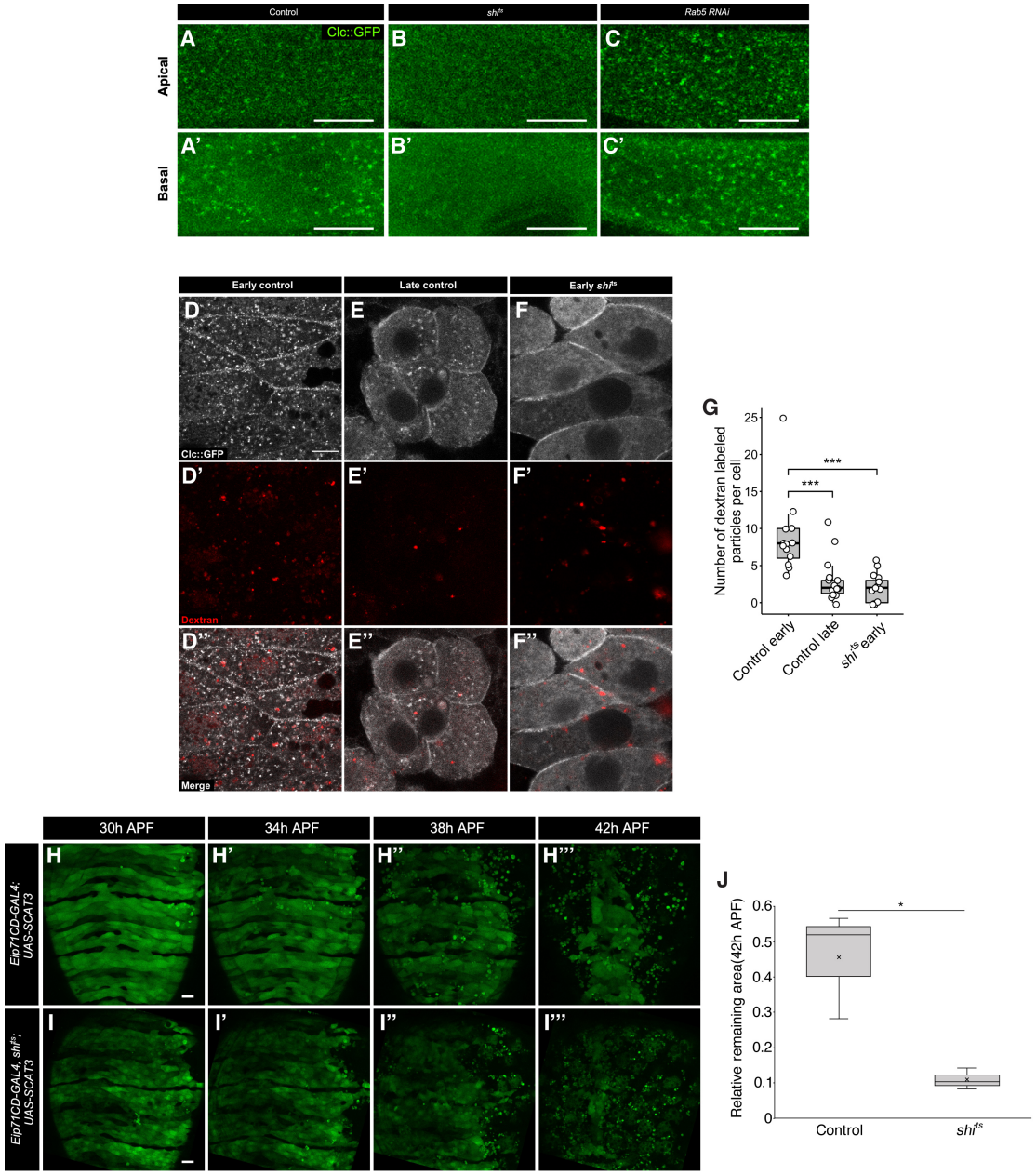

Figure S1. Endocytic activity reduces as tissue remodeling progresses during metamorphosis

(A-C) Clc::GFP puncta as a marker for endocytic activity in RT control (A), *shi*^{ts} expressing (B), and *Rab5* RNAi (C) LECs. Anterior is up. Scale bar: 10 µm. Note that the number of puncta was dramatically reduced for *shi*^{ts} expressing cells, and numerous smaller puncta accumulated for *Rab5* RNAi, which is consistent with the reported phenotype for *Rab5* inhibition (Bucci *et al.*, 1992).

(D-F) Dextran uptake for RT control at the early stage (D), the late stage (E), and *shi*^{ts} at the early stage (F). Clc::GFP (white) and dextran (red) are shown.

(G) Quantification of the number of dextran labeled vesicles per cell (control early: N = 13 cells, control late: N = 14, *shi*^{ts}: N =13 Mann–Whitney *U* test, ***$p < 0.001$.

(H-I) Time course of the LEC elimination for RT control (H) and *shi*^{ts} expressing (I) LECs under the control of an Eip71CD-GAL4 driver under the restrictive temperature at different time points indicated above. Anterior is up. Scale bar: 50 μm.

(J) Quantification of the area of GFP expression domain at the time point 42 hours APF relative to 30 hours APF. Student's t test. *$p < 0.05$. N = 4 pupae for each experiment.

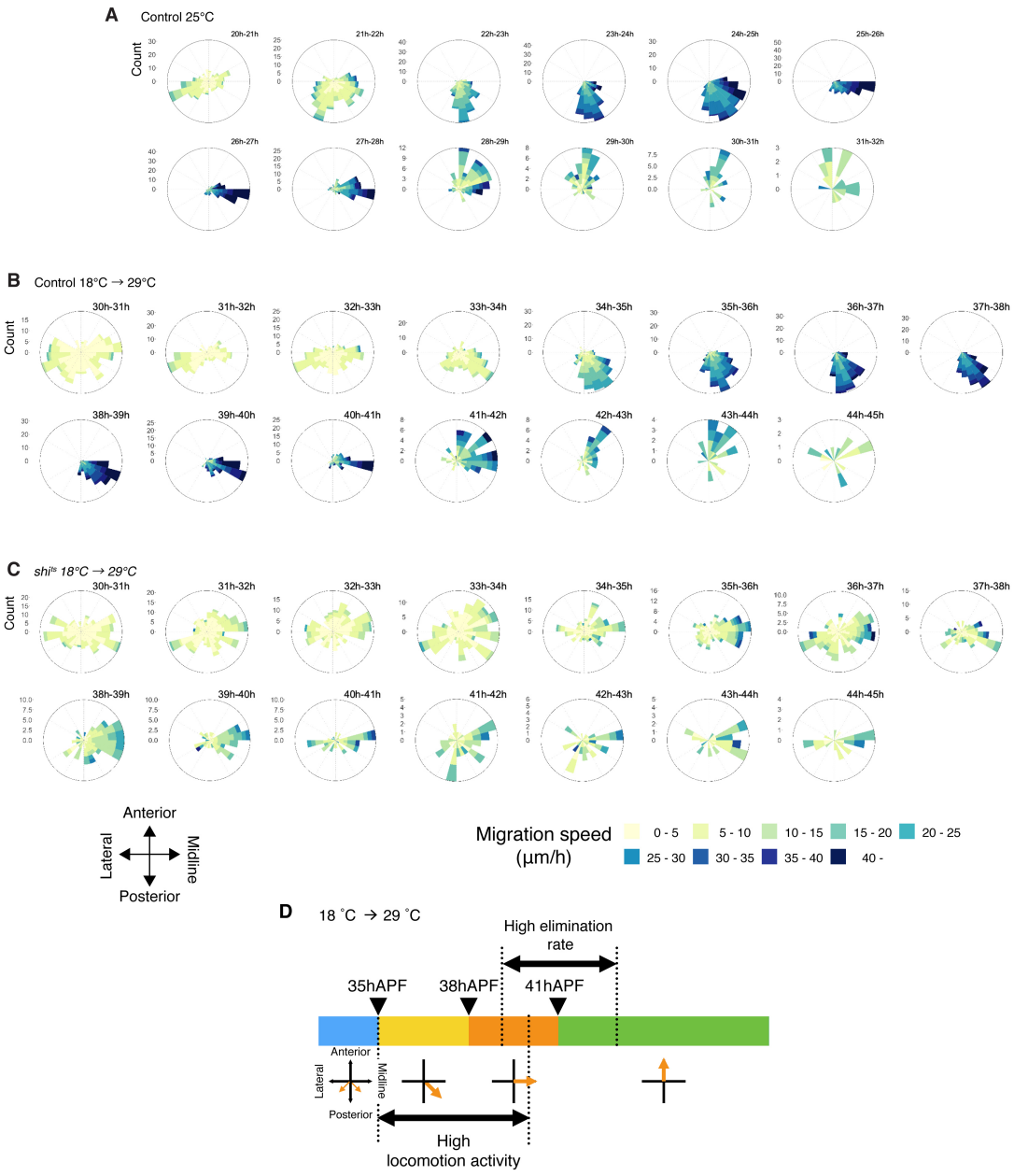

Figure S2. Reduction of endocytic activity affects migration of LECs

(A) Time course analysis of LEC migration orientation for control at 25°C .

(B-C) Time course analysis of LEC migration orientation for RT control (B) and *shi*^{ts} expressing (C) LECs under the restriction temperature regime.

(D) Timeline of the high elimination phase with respect to the migration pattern of the LECs under the restriction temperature regime. Color code (blue, yellow, orange and green) represents different developmental time windows from early to late stages based on the locomotion activity and orientation of migration. Times (after puparium

formation) of transition are indicated on top. Note that the developmental time windows in the restriction temperature regime roughly correspond to that of a standard condition (25˚C, Figure 1G). Orange arrows indicate orientation of the LEC migration at each time window. The time periods of high locomotion activity and high elimination rate are indicated below and above, respectively.

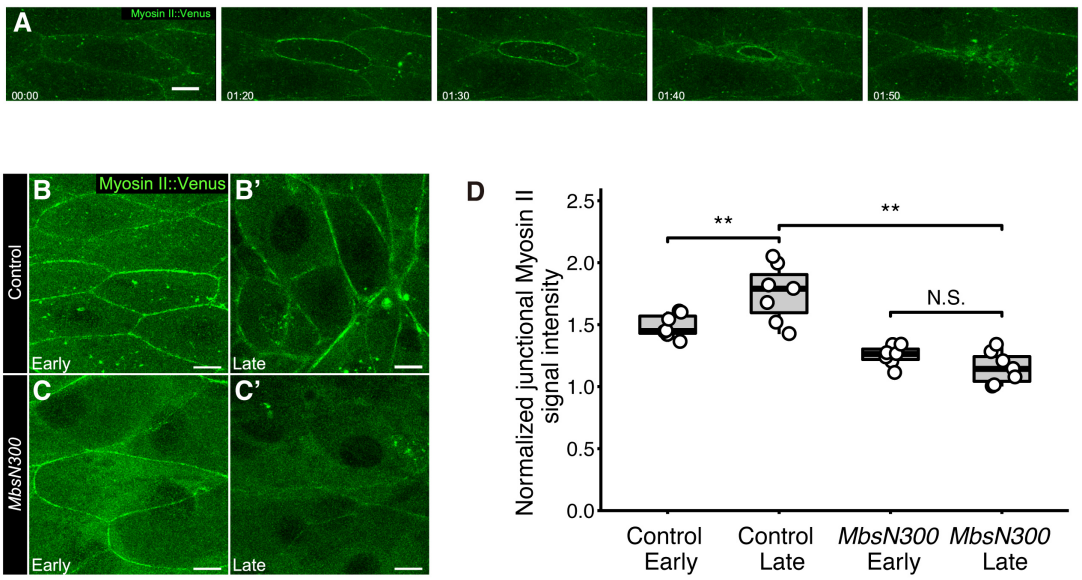

Figure S3. Reduction of cortical Myosin II in the late stage caused by the over-expression of *MbsN300*

(A) Still images for subcellular localization of myosin II tagged with Venus (MyoII::Venus) during apical constriction-driven cell elimination in RT control. Anterior is up. Scale bar: 10 μm.

(B-C) Subcellular localization of MyoII::Venus for control (B) and *MbsN300* expressing (C) LECs at the early (B, C) and late (B', C') stage. Note that the cortical localization of Myosin II is still visible at the early stage (C) but severely reduced at the late stage (C') upon over-expression of *MbsN300*.

(D) Signal intensity for MyoII::Venus at cell junctions normalized to that of cytoplasmic region for individual cells. Student's t-test, $^{**}p < 0.01$.

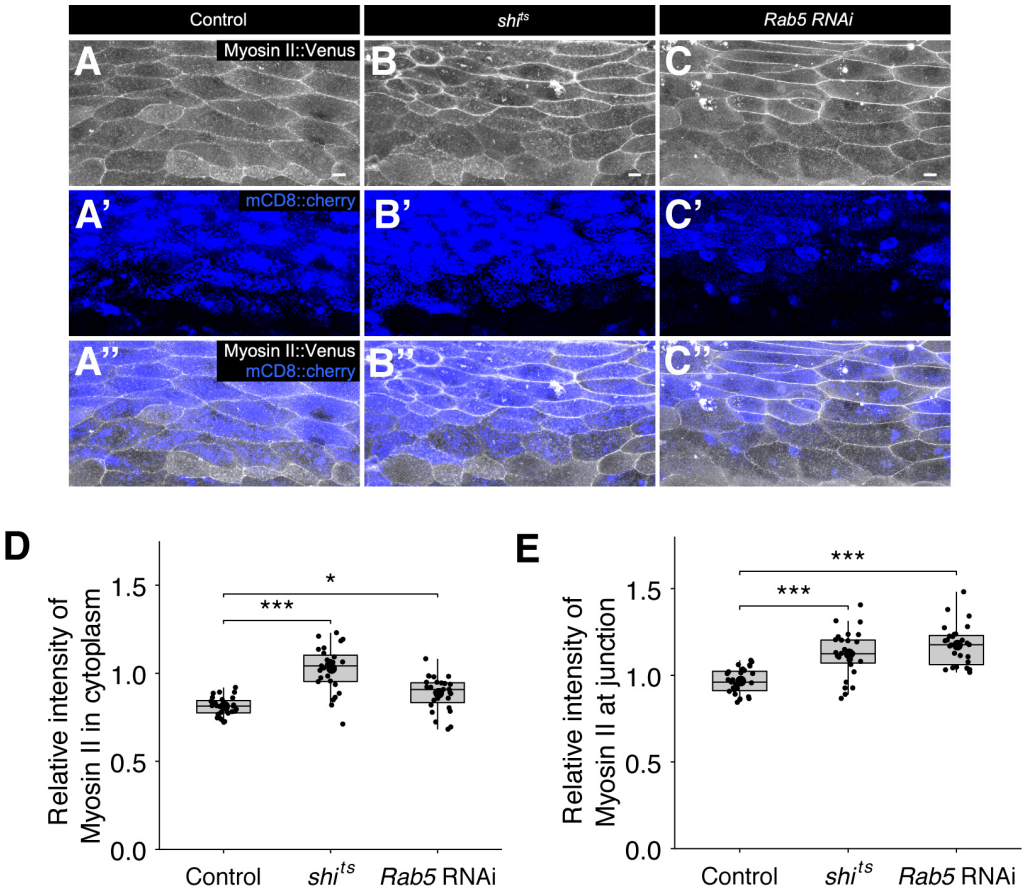

Figure S4. Myosin II levels are elevated in LECs with reduced endocytic activity

(A-C) Subcellular localization of MyoII::Venus in RT control (A), *shi*^{ts} expressing (B) and *Rab5* RNAi (C) LECs. Marker expression (mCD8::cherry) indicates the region of GAL4 expression (A', A'' B', B'' C', C''). Anterior is up. Scale bar: 10 μm.

(D-E) Quantification of signal intensity of MyoII::Venus in the RT control, *shi*^{ts} expressing and *Rab5* RNAi LECs relative to control region (*i.e.* non-GAL4 expression region) in each pupa for medial (D) and junctional (E) localization. One-way ANOVA followed by *post hoc* Games-Howell test. *$p < 0.05$, ***$p < 0.001$. N = 3 pupae, 27 cells each.

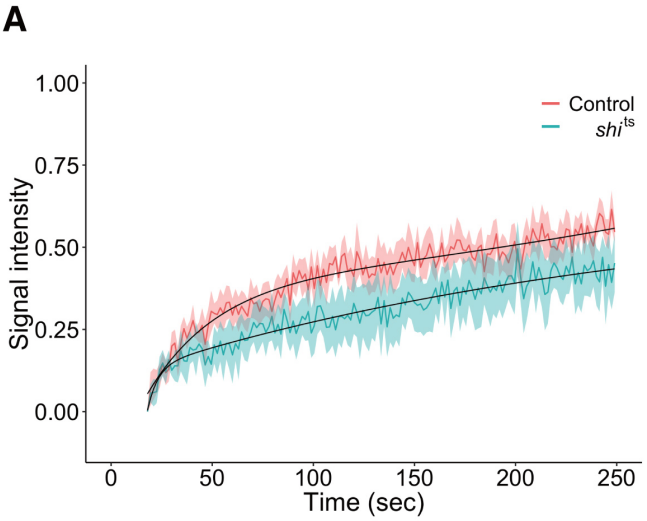

	Mobile fraction	T_{half} (sec)
Control	0.55	50
shi^{ts}	0.52	107

Figure S5. Turn-over of E-cadherin in control and *shi*^{ts} LECs

(A) Mobility of E-cadherin was analyzed by fluorescent recovery after photobleaching (FRAP) for RT control (red) and *shi*^{ts} expressing LECs (blue). A double exponential formula was used to fit the model to experimental results (black lines) to estimate the mobile fraction and the halftime of recovery T_{half}. E-cadherin::GFP was used for FRAP experiments. Staged control and *shi*^{ts} pupae were imaged by TCS SP8 confocal microscope (Leica) with 63× oil objective lens with 2.0x zoom, under 10-20% 488nm laser. 30-32h APF pupae were used for the early stage, and late stage pupae were 40-42h APF. An about 5 × 2 µm region was selected for photobleaching with 100% intensity 488 nm laser for 0.653 seconds. Manually selected non-fluorescence area and total fluorescence area were used for normalization for each cell. Images were acquired with 0.5 seconds time intervals. Obtained dataset were averaged and then analyzed by fitting a double exponential formula:

$$I(t) = I_0 - \alpha \cdot e^{-\beta \cdot t} - \gamma \cdot e^{-\delta \cdot t}$$

$$Mobile\ fraction = I_0, \qquad T_{half} = \frac{ln(2)}{\beta}$$

The mobile fraction and the T_{half} are indicated in the table. Control: N = 10, *shi*^{ts}: N= 9.

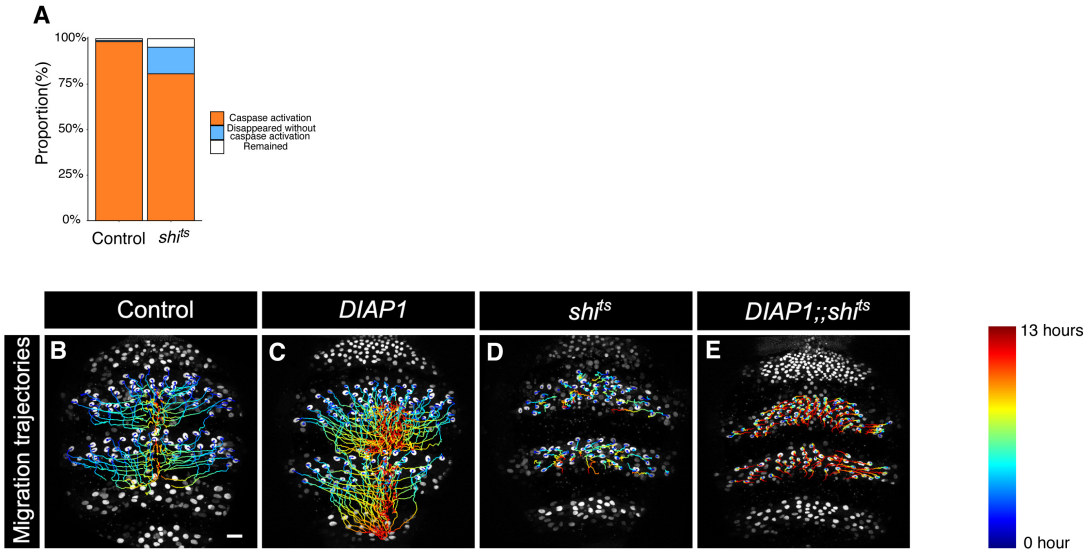

Figure S6. Caspase activation-associated LEC elimination and cell elimination independent migration of endocytic defective LECs

(A) Fraction of FRET signal positive cells among all dying cells for RT control and *shi*^{ts} expressing LECs.

(B-E) Migration trajectories of LECs for RT control (B), DIAP over-expressing (C), *shi*^{ts} expressing (D), and *shi*^{ts} and DIAP over-expressing (E) pupae under the restrictive temperature.

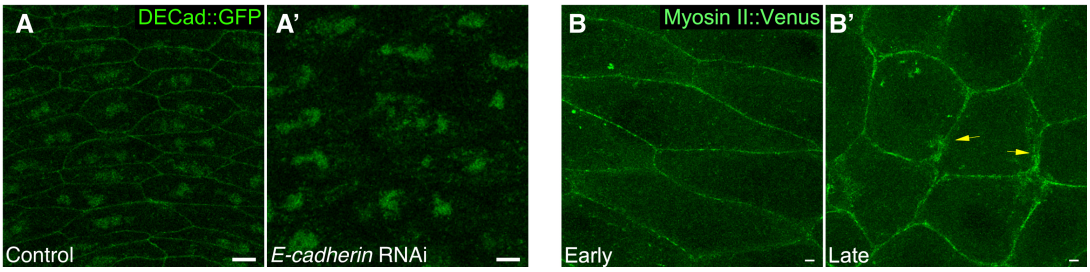

Figure S7. E-cadherin RNAi effectively reduces E-cadherin levels and Myosin II is not regulated by caspase activation

(A) E-cadherin::GFP in the LECs upon E-cadherin RNAi. Junctional E-cadherin signals are strongly reduced. Anterior is up. Scale bar: 10 μm.

(B) MyoII::Venus reorganization at the late stage is unaffected by the over-expression of *DIAP1*. Yellow arrows indicate thick cortical accumulation of MyoII::Venus. Anterior is up. Scale bar: 10 μm.

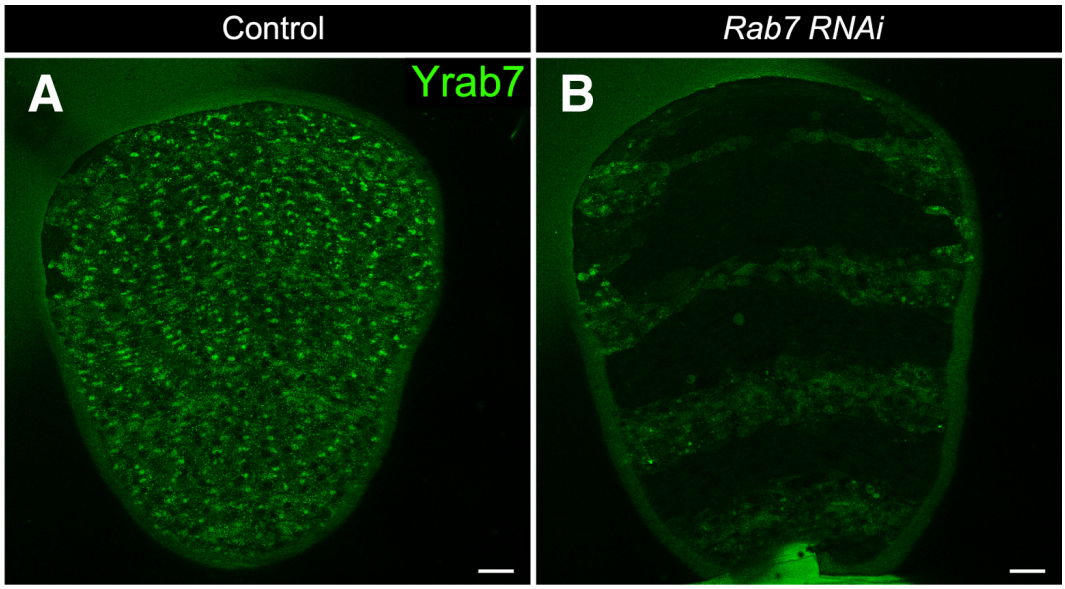

Figure S8. Reduction of Rab7 protein by *Rab7* RNAi

(A-B) Rab7::YFP knock-in (Dunst, Kazimiers, Eaton, *et al.*, 2015) for control (A) and *Rab7* RNAi (B) pupae. Anterior is up. Scale bar: 50 µm.

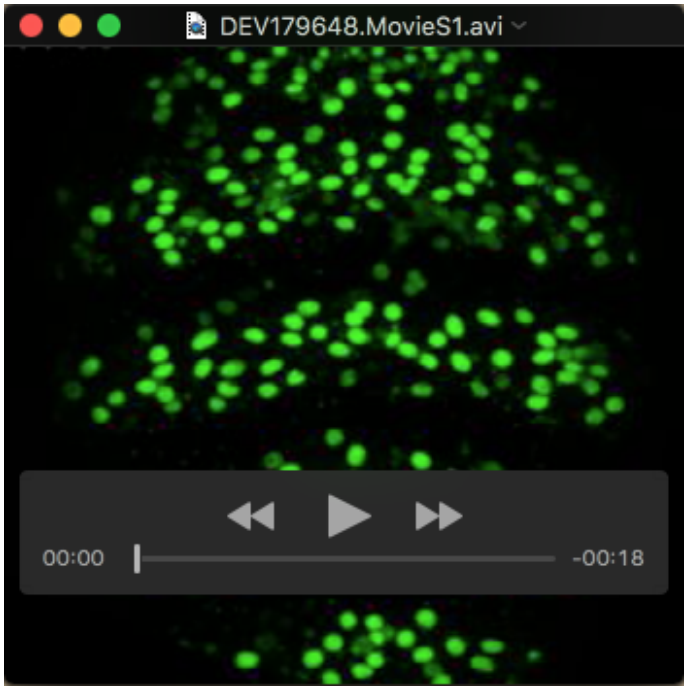

Movie 1. The elimination of LECs accelerates in the late stage of the tissue remodeling process

Live imaging of the elimination of the LECs, labeled by the nuclear localized CFP::Venus under the control of *pnr*-GAL4 driver at 25˚C. Dorsal view. Anterior is up. Scale bar: 50 μm. Time interval: 10 min.

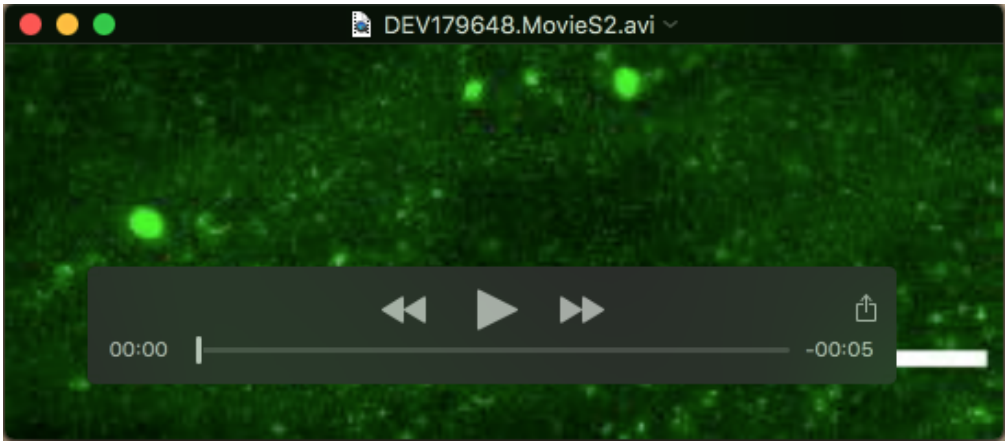

Movie 2. The number of Clc::GFP puncta reduces as tissue remodeling progresses

Live imaging of endocytic activity in the LECs using Clc::GFP as a marker. Although GFP signal is uniformly distributed in the cytoplasm, the number of GFP puncta gradually decreases over time. Note that eliminated cells also have much stronger accumulation of GFP puncta, which is the post-process of cell elimination and therefore irrelevant to the analysis of this study. Dorsal view. Anterior is up. Scale bar: 10 μm. Time interval: 5 min.

Movie 3. Expression of *shi*^{ts} in the LECs promotes cell elimination

Live imaging of the LEC elimination from pupae under the restrictive temperature (raised at 18˚C, then shifted to 29˚C at 6 hours before imaging) for RT control (left) and *shi*^{ts} expressing (right) LECs. Dorsal view. Anterior is up. Scale bar: 50 μm. Time interval: 10 min.

Movie 4. Induction of *Rab5* RNAi in the LECs promotes cell elimination

Live imaging of the LEC elimination from pupae under the restrictive temperature (raised at 18˚C, then shifted to 29˚C at 6 hours before imaging) for RT control (left) and *Rab5* RNAi (right) LECs. Dorsal view. Anterior is up. Scale bar: 50 μm. Time interval: 10 min.

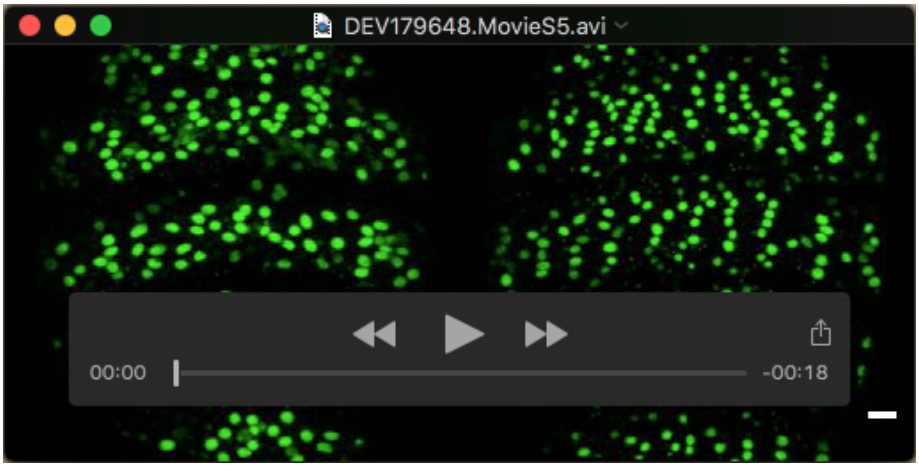

Movie 5. Over-expression of the Myosin II phosphatase *MbsN300* in the LECs diminishes the acceleration of cell elimination in the late stage

Live imaging of LEC elimination in pupa for control (left) and cells expressing Myosin phosphatase catalytic domain, *MbsN300* (right) at 25˚C. Dorsal view. Anterior is up. Scale bar: 50 μm. Time interval: 10 min.

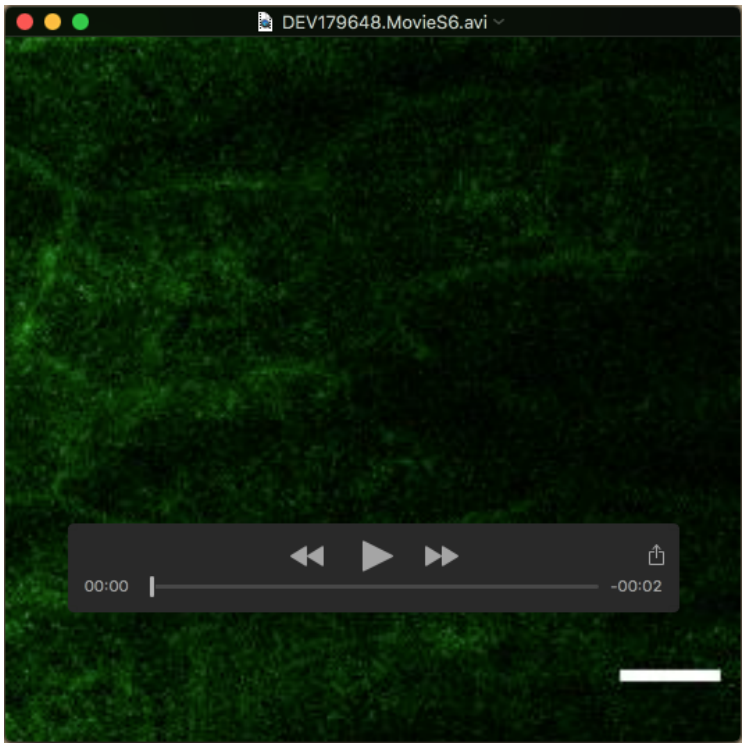

Movie 6. LECs in the early stage display Myosin II localization at the apical region

Z-slice stack of MyoII::Venus in the LECs at the early stage for RT control (30h APF). Scale bar: 10 μm. Z-slice interval: 0.75 μm.

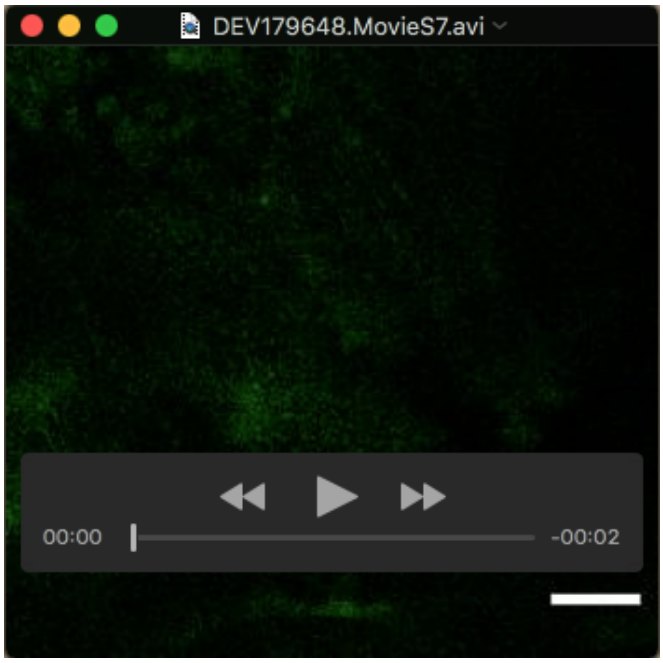

Movie 7. LECs in the late stage display strong Myosin II localization

Z-slice stack of MyoII::Venus in the LECs at the early stage for RT control (40h APF). Scale bar: 10 μm. Z-slice interval: 0.75 μm.

Movie 8. *shi*^{ts} expressing LECs in the early stage display strong Myosin II localization

Z-slice stack of MyoII::Venus in the LECs at the early stage for *shi*^{ts} (30h APF). Scale bar: 10 μm. Z-slice interval: 0.75 μm.

Movie 9. *shi*^{ts} expressing LECs in the late stage display strong Myosin II localization

Z-slice stack of MyoII::Venus in the LECs at the early stage for *shi*^{ts} (40h APF). Scale bar: 10 μm. Z-slice interval: 0.75 μm.

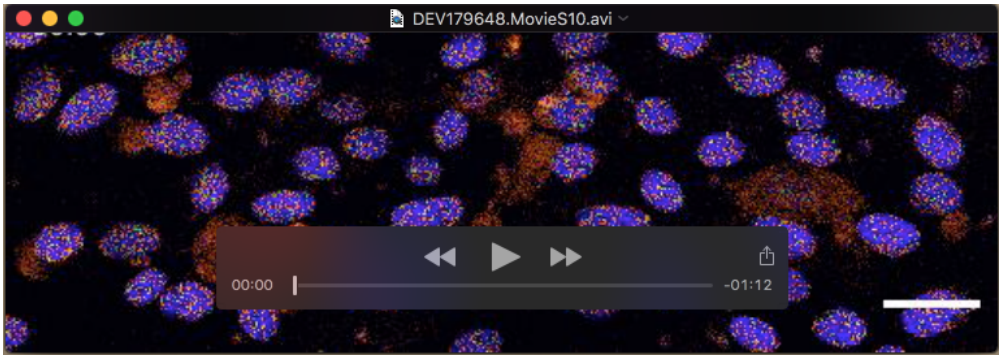

Movie 10. Caspase activation is observed before fragmentation of LECs in RT control and *shi*^{ts} expressing LECs

Live imaging of the FRET ratio of the nuclear localized SCAT3 caspase activation indicator (ECFP/Venus) for RT control LECs under the restrictive temperature. The higher FRET ratio indicates the higher caspase activity. Dorsal view. Anterior is up. Scale bar: 50 μm. Time interval: 100 sec.

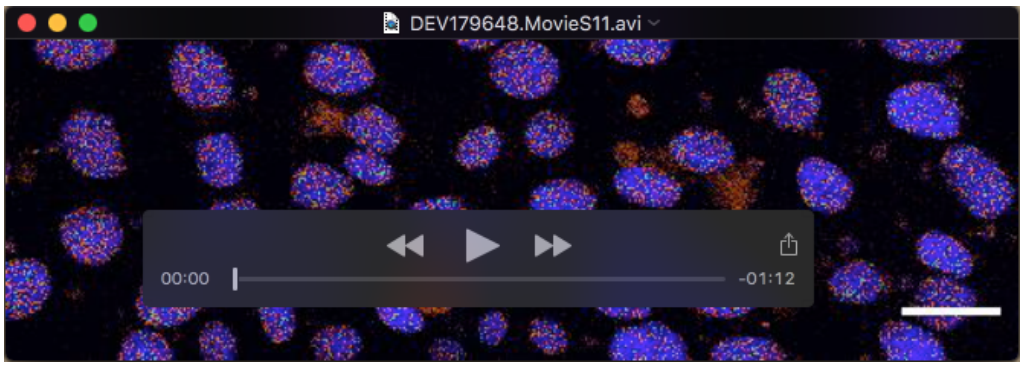

Movie 11. Caspase activation is observed before fragmentation of LECs in *shi*^{ts} expressing LECs

Live imaging of the FRET ratio of the nuclear localized SCAT3 caspase activation indicator (ECFP/Venus) for *shi*^{ts} expressing LECs under the restrictive temperature. The higher FRET ratio indicates higher caspase activity. Dorsal view. Anterior is up. Scale bar: 50 μm. Time interval: 100 sec.

Movie 12. Over-expression of *DIAP1* suppresses cell elimination caused by expressing *shi*^{ts} in the LECs

Live imaging of LEC elimination from pupae under the restrictive temperature for *shi*^{ts} expressing (left) and *DIAP1* and *shi*^{ts} expressing (right) pupae. Dorsal view. Anterior is up. Scale bar: 50 μm. Time interval: 10 min.

Movie 13. Induction of *E-cadherin* RNAi in the LECs promotes cell elimination

Live imaging of LEC elimination for control (left) and *E-cadherin* RNAi (right) LECs at 25˚C. Dorsal view. Anterior is up. Scale bar: 50 μm. Time interval: 10 min.

Movie 14. Over-expression of *DIAP1* suppresses cell elimination caused by the reduction of *E-cadherin* in the LECs

Live imaging of the LEC elimination for control (left) and *DIAP1* and *E-cadherin* RNAi (right) LECs at 25˚C. Dorsal view. Anterior is up. Scale bar: 50 μm. Time interval: 10 min.

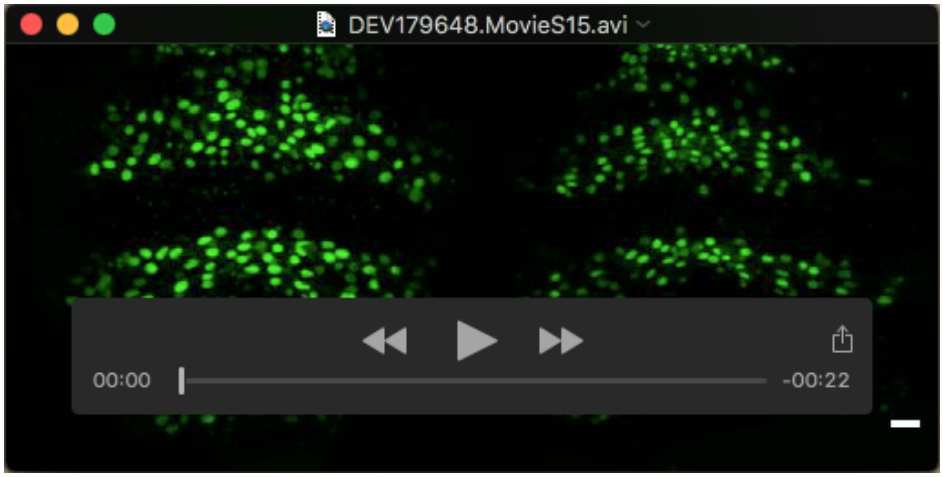

Movie 15. Over-expression of *E-cadherin* moderates increased cell elimination caused by expressing *shi*^{ts} in the LECs

Live imaging of LEC elimination under the restrictive temperature for *shi*^{ts} expressing (left) and *shi*^{ts} and *E-cadherin* over-expressing (right) LECs. Dorsal view. Anterior is up. Scale bar: 50 μm. Time interval: 10 min.

Movie 16. Induction of *Rab7* RNAi in the LECs promotes cell elimination

Live imaging of LEC elimination for control (left) and *Rab7* RNAi (right) LECs at 25˚C. Dorsal view. Anterior is up. Scale bar: 50 μm. Time interval: 10 min.